# Curvature-induced interchange mode in an axisymmetric plasma

Michael Wickham

*Physics Department, University of California, Irvine, California 92717*

Guy Vandegrift

*Department of Electrical Engineering, University of California, Berkeley, California 94720*
(Received 11 May 1981; accepted 30 October 1981)

A theoretical and experimental description of the curvature-induced electrostatic interchange mode in a simple mirror confined low-$\beta$ plasma is given. The frequency, growth rate, and nonflute-like effects have been measured and compared with theory. Effects due to radial electric field, finite ion Larmor radius, line-tying, wall radius, and parallel electron response are discussed.

## I. INTRODUCTION

The interchange mode in a magnetic mirror confined plasma is driven by magnetic field curvature which varies between being stabilizing and destabilizing as one moves along a field line. The effects of conducting boundaries can have a profound effect on the frequency and growth rate of this mode. We will show that the radial position of a conducting wall as well as the conductivity of the plasma terminator (end plate) can greatly influence the mode. We were able to change the conductivity of the plasma terminator to two different values and observe the influence of line-tying on the frequency and growth rate of the interchange mode. We also observed a finite $k_z$. In the pure $k_\parallel = k_z = 0$, flute limit, the mode is electrostatic with a perturbed potential $\varphi_1$ which is constant along the magnetic field. Because the interchange mode in the typical magnetic mirror is nearly flute-like, it is possible to achieve overall stability by modifying only a portion of the field. Possibilities include quadrupole fields, hot ion plugs, hot electron plugs, and cusps.

An interchange mode having a small $k_z$ not equal to zero may be less stable than a flute mode because it can have a larger amplitude where the curvature is bad. The most serious finite $k_z$ effect for a reactor is probably the electromagnetic ballooning mode, which is a coupling between the Alfvén wave and the interchange mode. However in low-$\beta$ experiments, and in reactors with large axial density gradients and electric fields, the possibility of electrostatic finite $k_z$ effects exists. ($\beta$-plasma pressure/magnetic pressure.)

In our experiment we observe the $m = 1$ mode; however, we derive a general dispersion relation which is valid for all $m$ numbers. We investigate, theoretically, the influence that a conducting coaxial wall and end wall have on the interchange mode. We could not experimentally verify all of the effects indicated by our theoretical derivations; however, the results, in the region of parameter space available to us, agree remarkably well with our calculations.

We shall consider a $\beta = 0$, axisymmetric plasma with a uniform magnetic field, $B_0\hat{z}$. The temperature is uniform, and the density is $n_0(z)\exp(-r^2/r_0^2)$, where $r_0$ is independent of $z$.

Although we treat the magnetic field as uniform, the inhomogeneities in the actual magnetic field produce drifts. To describe these we define a $z$ dependent parameter, $\omega_c^2(z)$, which is positive in regions of destabilizing curvature and negative in regions of stabilizing curvature. Physically $\omega_c$, appropriately averaged along $z$, is the classical growth rate of the interchange instability neglecting finite Larmor radius stabilization and the influence of conducting boundaries. The magnitude of $\omega_c$ is related to the actual magnetic field $B$ by $|\omega_c| = v_i |d \ln B/dz|$, where $v_i = (2T_i/m_i)^{1/2}$ and $T_i$ and $m_i$ are the ion temperature and mass, respectively. If $T_i \gg T_e$, the curvature may be replaced by a "gravitational" force on the ions, which produces an azimuthal drift velocity $-(r\omega_c^2/\Omega_i)\hat{\theta}$, where $\Omega_i = eB/m_i c$ is the cyclotron frequency. We also allow for a rigid rotor rotational velocity, $r\omega_E\hat{\theta}$ on both electrons and ions due to a radial electric field.

In Sec. II, we derive a dispersion relation that neglects finite $k_z$ effects, but includes line tying. In Sec. III, we discuss the finite $k_z$ effects. In Sec. IV, the experiment is described, and in Sec. V, we present experimental results that confirm several aspects of the theory.

## II. DISPERSION RELATION

The perturbed electrostatic potential is assumed to be $\varphi_1(r)\exp(-i\omega t + im\theta)$. The boundary condition is that $\varphi_1 = 0$ when $r = r_w$, where $r_w$ is the wall radius (which is assumed to be conducting). Also, $\varphi_1$ must vanish at the endplates at $z = \pm L$. We assume $\varphi_1$ is nearly constant along $z$, except for a small sheath region near $z = \pm L$. To derive the dispersion relation we will impose quasineutrality ($\rho_i + \rho_e \cong 0$) which is valid if $\epsilon_\perp \gg 1$; $\epsilon_\perp$ is the cold plasma dielectric constant and $\rho_i, \rho_e$ are the ion and electron perturbed charge densities, respectively. In order to calculate $\omega$ we will make the pure flute, $k_z = 0$, approximation. This is justified by the fact that $k_z \approx 0$ as we shall see later.

First consider the ions. When $T_{i\perp} \gg T_{i\parallel}$, we may neglect parallel ion motion completely and consider a two-dimensional distribution of ions in an electrostatic field. We begin with the finite Larmor radius fluid equations derived by Rosenbluth and Simon,[1]

 0031-9171/82/010052-07$1.90  

$$D\rho_m + (1/\Omega^2)\nabla\cdot(\rho_m D\mathbf{G} - D\nabla p) = 0\,, \tag{1}$$

$$D\rho = 0\,, \tag{2}$$

where $D \equiv \partial/\partial t + \mathbf{V}\cdot\nabla$ and $\mathbf{V} = (\mathbf{G}\times\hat{z}/\Omega; \rho_m$ is the mass density, $p$ is the pressure, and $\mathbf{G}$ represents the acceleration of all forces other than the $\mathbf{v}\times\mathbf{B}$ force. These equations can be linearized to yield a relationship between the perturbed ion charge density $\rho_i(r)$ and $\varphi_1(r)$,

$$\rho_i = R_i\varphi_1\,, \tag{3}$$

where

$$R_i = \frac{\epsilon_\perp}{4\pi r_0^2}\left(\frac{2m\Omega_i}{\bar{\omega}} - \frac{2(\bar{\omega}+m\omega_D)}{\bar{\omega}}\hat{\beta} - \frac{2(\omega^2+m^2\omega_c^2)}{\bar{\omega}^2}\right), \tag{4}$$

and $\hat{\beta}$ is the differential operator

$$\hat{\beta} = -\frac{r_0^2}{2}\frac{\partial^2}{\partial r^2} + \left(r - \frac{r_0^2}{2r}\right)\frac{\partial}{\partial r} + \frac{m^2 r_0^2}{2r^2} - 1\,, \tag{5}$$

$\bar{\omega} = \omega - m\omega_E$, $\omega_D = 2v_i^2/r_0^2\Omega_i$ is the ion diamagnetic drift frequency, and $\epsilon_\perp = \omega_i^2/\Omega_i^2$. $\omega_i^2 = 4\pi ne^2/m_i$ is the ion plasma frequency and has the same $r$ and $z$ dependence as the unperturbed density $n_0(z)$. The first term in Eq. (4) arises from the $\mathbf{E}\times\mathbf{B}$ drift due to the perturbed field. The other two terms are corrections valid to first order in the small parameters $\omega_c/\Omega_i$, $\omega/\Omega_i$, $\omega_D/\Omega_i$, and $\omega_E/\Omega_i$. These small parameters represent effects due to curvature, polarization drift, finite Larmor radius, and a radial electric field, respectively. This response is the cylindrical generalization of the slab model derived by Jukes.[2] We shall show that $\hat{\beta}$ may be replaced by the eigenvalue $\lambda$. This makes Eq. (4) as simple, but more realistic than the slab model. The curvature term $\omega_c$ is obtained from an appropriate average.

The electron response is more difficult to treat because motion in the $\hat{z}$ direction is important. Motion perpendicular to $\hat{z}$ is simple $\mathbf{E}\times\mathbf{B}$ drift and produces a contribution to the electron response equal and opposite to the first term in Eq. (4). The other two terms in Eq. (4) are smaller by the mass ratio for the electron response and will be neglected. If the plasma is terminated by a conducting endplate, then a source term must be included in the electron response. We may apply the model of Kunkel and Guillory[3] and Prater[4] to a rotating plasma since both the centrifugal and coriolis forces produce corrections of order $\omega_E/\Omega_e$, where $\Omega_e$ is the electron cyclotron frequency. Thus, the $\mathbf{E}\times\mathbf{B}$ drifts and the line tying effect yields the two-dimensional electron charge density response

$$\rho_e = \frac{\epsilon_\perp}{4\pi r_0^2}\left(-\frac{2m\Omega_i}{\bar{\omega}} - \frac{4i\nu}{\bar{\omega}}\right)\varphi_1\,, \tag{6}$$

where

$$\nu \sim M_i v_i \Omega_i^2 r_0^2/4kT_e l_m\,, \tag{7}$$

measures the line-tying effect. A large value of $\nu$ indicates good line-tying. Here, $v_i$ is the ion thermal velocity near the plasma terminator and $l_m$ is the length of the mirror. Equations (6) and (7) are derived from particle drift equations in the appendix. The line-tying parameter $\nu$ is also given physical significance there. We now impose quasineutrality ($\rho_i + \rho_e \cong 0$) and combine Eqs. (3) and (6) to yield the differential equation

$$\varphi_1'' + \frac{1}{r}\varphi_1' - \frac{m^2}{r^2}\varphi_1 - \frac{2}{r_0^2}[r\varphi_1' - (1+\lambda)\varphi_1] = 0\,. \tag{8}$$

This may also be written as the eigenvalue equation $\hat{\beta}\varphi_1 = \lambda\varphi_1$, where

$$\lambda = -\left(\frac{\bar{\omega}^2 + 2\bar{\omega}(m\omega_E + i\nu) + m^2(\omega_c^2 + \omega_E^2)}{\bar{\omega}(\bar{\omega} + m\omega_D)}\right). \tag{9}$$

Primes denote differentiation with respect to $r$. Equation (8) can be put in the form of Whittaker's equation[5] and is similar to the equation solved by Rosenbluth *et al.*,[6] but includes finite wall radius and line-tying. The constant $\lambda$ is determined by requiring that $\varphi_1(r) = 0$ at $r = r_w$; $\lambda$ is a real constant. Equation (8) can be put in Hermitian form, and the eigenvalues of the Hermitian operators are real. The fact that Eq. (8) can be put into Hermitian form is a result of the form of the differential operator and the boundary conditions. Figure 1 shows the dependence of $\lambda$ on wall radius $r_w$ for the lowest-order modes, ($q$ is the number of times $\varphi_1$ equals zero between $r = 0$ and the wall; $q = 0$, $m = 1$ being the lowest-order mode). As the wall radius $r_w$ goes to infinity, $\lambda \to m + 2q - 1$, where $m$ and $q$ are azimuthal and radial mode numbers. Equation (9) is quadradic in $\bar{\omega}$ and has the solution

$$\bar{\omega} = [-B \pm (B^2 - AC)^{1/2}]/A\,, \tag{10}$$

where

$$A = 1 + \lambda\,, \tag{11}$$

$$B = m\omega_E + i\nu + \lambda m\omega_D/2\,, \tag{12}$$

and

$$C = m^2(\omega_E^2 + \omega_c^2)\,. \tag{13}$$

In the limit of infinite wall radius for the $m = 1$, $q = 0$ mode this reduces to

$$\omega = -i\nu \pm i(\nu^2 + \omega_c^2 - 2i\nu\omega_E)^{1/2}\,. \tag{14}$$

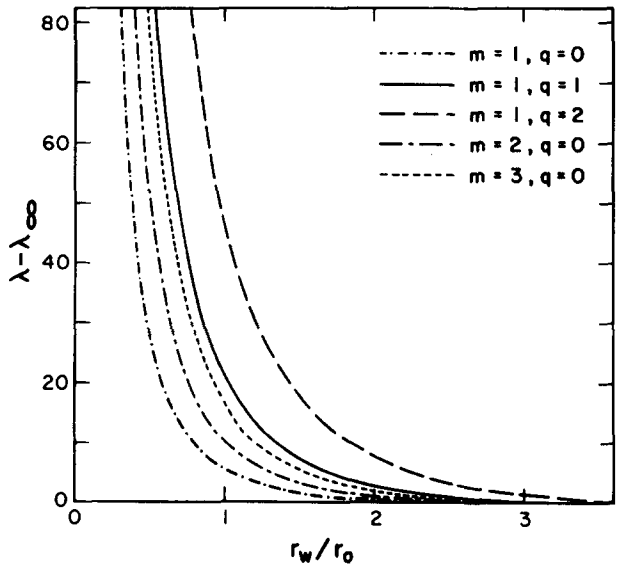


FIG. 1. $\lambda$ vs the ratio of wall radius $r_w$ to plasma radius $r_0$. $\lambda_\infty = m + 2q - 1$ is the limit when the wall is at infinity.

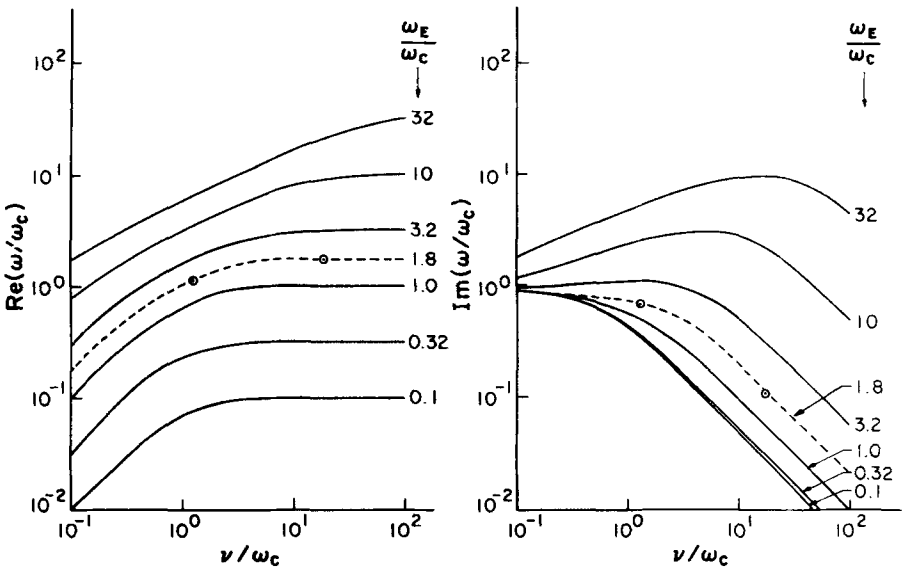


FIG. 2. Real frequency and growth rate of the $m=1$ mode vs line-tying for different radial electric fields ($\omega_E$). $R_e\,\omega \to \omega_E$ and Im $\omega \to 0$ as $\nu \to \infty$; Re $\omega \to 0$ and Im $\omega \to \omega_c$ as $\nu \to 0$. Note the destabilization by partial line tying for $(\omega_E/\omega_c) \gtrsim 3.2$. The dashed lines correspond to the experimentally determined value of $(\omega_E/\omega_c) = 1.8$. The circles on those lines indicate the two values of $\nu$ which we could explore experimentally.

Figure 2 shows $\omega$ versus $\nu$ for various values of $\omega_E$. When $\omega_E = 0$, line-tying always reduces the growth rate which approaches $\omega_c^2/2\nu$ when $\nu \gg \omega_c$. When $\omega_E$ is not zero, the real part of $\omega$ approaches $\omega_E$ when $\nu \gg \omega_c$. Line-tying has an unexpected effect on the mode when $\omega_E \gtrsim \omega_c$. The growth rate is increased for moderate values of $\nu$. The radial electric field can drive the $m=1$, $q=0$ mode unstable only when an endplate or conducting wall[7] is present.

## III. FINITE $k_z$ EFFECTS

A physical explanation for the electrostatic finite $k_z$ effect is as follows: By quasineutrality, $\rho_e + \rho_i = 0$ for all $z$. The perturbed charge densities have different $z$ dependencies and if the system varies along $z$, then the electron and ion currents will not cancel for all $z$. Thus, quasineutrality implies a parallel perturbed electron current. The parallel electric field required to drive this current implies that $\varphi_1$ must vary along $z$. Since $E = -\nabla\varphi_1$, the perpendicular perturbed electric field must depend on $z$. The case of highly collisional electrons has been treated using fluid equations.[8] We shall treat the case of collisionless electrons with transit time across the machine much less than $\omega^{-1}$ or $\omega_E^{-1}$.

When the electron mean-free-path is short compared with the plasma length, the problem can be solved using fluid equations.[8] However when the electrons are collisionless, a kinetic, nonlocal electron response must be obtained. We shall illustrate this with an idealized model which does not include line-tying: Assume that the electrons are confined along $z$ by perfectly reflecting walls at $z = \pm L$. Assume also that the unperturbed density and electrostatic potential are independent of $z$ for $-L < z < L$. If the electron transit time across the length of the plasma is much less than $\omega_E^{-1}$ or $\omega^{-1}$, we may assume that the electrons come into thermal equilibrium with respect to $\varphi_1(z)$.

We will first calculate the parallel response $\rho_{e\parallel}$, which is the electron charge density due to a force field with only a $\hat{z}$ component. Next, we will calculate the perpendicular charge density response $\rho_{e\perp}$, which is the response to the force with no $\hat{z}$ component.

To calculate the parallel response we consider a perturbed force field $\mathbf{F}_\parallel = e\hat{z}\partial\varphi_1(r)/\partial z$. Since we ignore perpendicular forces to calculate $\rho_{e\parallel}$, the number of electrons on a given field line at $(x, y)$ will remain constant. The $z$ dependence of $\rho_{e\parallel}$ is determined by the fact that $\varphi_1$ changes slowly enough in time so that the electrons remain in adiabatic equilibrium with $\varphi_1$. The result for the perturbed plus unperturbed electron charge density, $\rho = \rho_0 + \rho_1$, is

$$\rho_0 + \rho_1 \cong \rho_0 \exp\{[e\varphi_1(z) - e\langle\varphi_1(z)\rangle]/T_e\}\,, \tag{15}$$

$$\rho_1 \equiv \rho_{e\parallel} \cong (-1/4\pi\lambda_e^{\,2})(\varphi_1(z) - \langle\varphi_1(z)\rangle)\,, \tag{16}$$

$$\langle\varphi_1(z)\rangle = \frac{1}{2L}\int_{-L}^{L}\varphi_1(z)dz\,, \tag{17}$$

where $\lambda_e^{\,2} = T_{e\parallel}/4\pi n_0 e^2$. Equation (15) is the Maxwell-Boltzmann law with a constant added to $\varphi_1(z)$ to ensure that the total perturbed charge along each field line vanishes: $\int \rho_1\, dz = 0$.

To calculate the perpendicular response, we assume a force field on the electrons $\mathbf{F}_\perp = e(\hat{x}\partial/\partial x + \hat{y}\partial/\partial y)\varphi_1(\mathbf{r})$. From the E×B drift equations, we may calculate the total number of electrons that drift onto a field line located at $(x, y)$. The $z$ dependence of this perturbed charge is determined by the fact that there are no parallel forces: $\rho_{e\perp}$ is independent of $z$. The perpendicular response resembles Eq. (6) without line-tying

$$\rho_{e\perp} = -(\epsilon_\perp/4\pi r_0^{\,2})\langle 2m\Omega_i\varphi_1/(\omega - m\omega_E)\rangle, \tag{18}$$

where the bracket indicates a $z$ average, and we allow $\omega_E$ and $\varphi_1$ to depend on $z$. It is necessary to take the average in Eq. (18) because the electron transit time along the machine is much less than $\omega^{-1}$. $\rho_{e\perp}$ is then a measure of the net amount of charge due to the perpendicular force field.

To obtain the actual response, we note that $\rho_e = \rho_{e\parallel}$

$+\rho_{e\perp}$ since $e\nabla\varphi_1 = F_\parallel + F_\perp$, and the response is linear in F. From Eqs. (16) and (18):

$$\rho_e = \frac{-\epsilon_\perp}{4\pi r_0^2}\left\langle \frac{2m\Omega_i\varphi_1(z)}{\omega - m\omega_E(z)} \right\rangle - \frac{1}{4\pi\lambda_e^2}[\varphi_1(z) - \langle\varphi_1(z)\rangle]. \tag{19}$$

From Eqs. (4) and (19) we may impose quasineutrality to obtain the $z$ dependence of $\varphi_1$, assuming that we may replace the operator $\hat{\beta}$ in Eq. (5) by its eigenvalue $\lambda$. For the $m=1$, $q=0$ mode with $r_w=\infty$ one obtains

$$\varphi_1(z) = \frac{\langle\varphi_1\rangle - \langle 2\Omega_i\varphi_1/(\omega-\omega_E)\rangle\delta}{1 - \delta\{2\Omega/(\omega-\omega_E(z)) + 2[\omega^2+\omega_c^2(z)]/(\omega-\omega_E(z))^2\}},$$

where $\delta \equiv \epsilon_\perp\lambda_e^2/r_0^2$ is a small number. If we assume that the mode is nearly flute like, we may Taylor expand the weak $z$ dependence of $\varphi_1$ as approximately $\varphi_1/|\varphi_1| \approx 1+\chi(z) \approx \exp[\chi(z)]$, where the complex phase is given by:

$$\chi \approx \delta\left(\frac{2\Omega_i}{\omega-\omega_E(z)} + \frac{2[\omega^2+\omega_c^2(z)]}{[\omega-\omega_E(z)]^2}\right) \equiv -i\int k_z(z)dz. \tag{20}$$

The real part of $\chi$ gives the amplitude variation of $\varphi_1(z)$, while variations in the imaginary part of $\chi$ give the phase lag between two values of $z$. From Eq. (20) we see that variations in either the curvature, or the radial electric field can cause a finite $k_z$. If the radial electric field does vary along $z$, it will dominate since the first term in Eq. (20) is much larger than the second term.

## IV. THE EXPERIMENT

The experiment was performed on the University of California, Irvine Q machine[9] (Fig. 3). The magnetic field was changed from the usual solenoidal field to a simple axisymmetric mirror with a field ratio of 2.53. The $B$ field configuration used is also shown in Fig. 3; the $B$ at midplane was 3 kG. The plasma radius $r_0$ at midplane was 2.8 cm. To insure that the plasma remain collisionless the density was not higher than $1-5\times10^9$ cm$^{-3}$ yielding an electron mean-free-path of several machine lengths. The background pressure was approximately $3\times10^{-7}$ Torr.

The Ba Q machine plasma was heated by inductive coil excitation[10] at the ion cyclotron frequency at midplane resonance. The plasma was heated from an initial perpendicular temperature of 0.25 eV to a final temperature of 3.5 eV; however, the parallel ion temperature did not change. The coil used was one wavelength with five filaments in series with a length of 65 cm. The calculated fields were approximately 0.1 V/cm. The parallel and perpendicular ion velocity distributions were optically determined using laser-induced resonance fluorescence.[11]

Once heated, the plasma from the source was cut off by a high transparency fine mesh grid placed between the source and the mirror region. The grid was biased 2 V below the plasma potential to repel electrons, and the ions did not travel very far beyond the grid because of space charge. A second grid between the first grid and the mirror region acted as a buffer to separate the first grid from the mirror confined plasma. The experiment was repeated at a rate of 10 sec$^{-1}$.

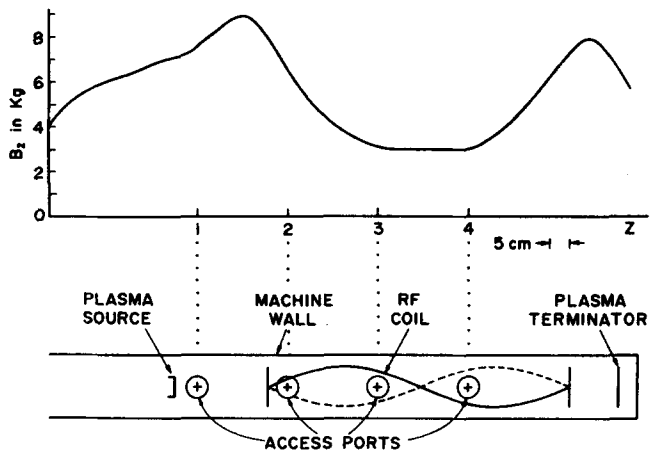


FIG. 3. Schematic diagram of the experimental apparatus and the magnetic field configuration.

The plasma was terminated by a floating molybdenum endplate. If the endplate was not heated, it was quickly coated with barium and became a poor conductor. By heating the endplate, we could clean it and create a partially line-tied plasma. We could examine only two states of the end plate, cold, coated with barium, or heated to remove the barium. The transition from one state to the other was unstable, and it was not possible to experimentally examine any intermediate states. In this manner we could control the amount of line-tying to a greater degree than most mirror experiments where the plasma is much more energetic and it is impossible to eliminate line-tying. Energetic plasma bombarding the plasma terminator can create a low-energy plasma which can line-tie the plasma.

Plasma potential profiles were measured with a floating Langmuir probe. These profiles were best fit to a parabola, $\varphi_0 = \alpha r^2$, $\omega_E$ was thus determined, $\omega_E = cE/rB = -2\alpha/B$. At $t=0$ the potential profile was flat in the center and dropped abruptly at the edge. The profile very quickly ($t \geq 200$ $\mu$sec) became parabolic. $\omega_E$ at these times was thus found to be $6.5\times10^3$ rad sec$^{-1}$.

The mode frequency was determined with four probes, each separated by 90° and placed in the mirror valley at $r=4$ cm. Finite $k_z$ effects were determined by simultaneous measurements at the midplane and throat of the mirror. Density profiles, mode frequency, and $k$ parallel measurements were made with probes, which were biased to collect ion current far into the saturation region in order to minimize error due to changes in the plasma potential.

The growth rate of the mode was determined by using time resolved vertical and horizontal density profiles of the plasma at midplane. This was possible because the mode was quite reproducible. The growth rate was estimated by measuring the initial displacement and velocity of the plasma. Since the early time behavior is given by $r = Ae^{\gamma t} \approx A + A\gamma t$, the initial velocity is related to the growth rate $\gamma$, by $V_0 = A\gamma$. The initial displacement $A$ is due to the nonuniformities inherent in the plasma production. We estimate $A$ to be 1 cm.

## V. THE RESULTS

The $m=1$ interchange mode evolution is shown in Fig. 4. The plasma column passes through the stationary probes in the sequence 2, 1, 4, 3, 2, and 1. As the plasma column rotates and moves radially outward different parts of it strike the stationary probes. Hence, the amplitudes of the probe signals vary in time. The real frequency $\omega_r$ was determined to be approximately $3.5\times10^3$ rad sec$^{-1}$ as determined by the dotted line in Fig. 4. The growth rate was found to be $2\times10^3$ rad sec$^{-1}$. If we assume that when the plasma terminator was cold there was no line-tying, $\nu=0$, then Eq. (10) reduces to

$$\omega_r \cong \lambda(\omega_E - \omega_D/2),$$

and

$$\gamma \approx \omega_c .$$

For the experimental wall position $\lambda=0.05$. This would make $\omega_r=-3.0\times10^2$ rad sec$^{-1}$ and $\gamma\approx3.6\times10^3$. This $\omega_r$ is too small and the wrong sign; also, the observed growth rate was much smaller than indicated here. These facts indicate that $\nu\neq0$, i.e., there was some line-tying. If we use Eq. (10) to find what value of $\nu/\omega_c$ best fits our observations, we find that $\nu/\omega_c=1.28$, which would give $\omega_r=4.1\times10^3$ rad sec$^{-1}$ and $\gamma=2.3\times10^3$ rad sec$^{-1}$.

These values are within 18% of the observed values and correctly predict the direction of propagation which was in the electron diamagnetic drift direction due to the direction of the radial electric field. In order to further investigate the effect of line-tying, we increased the conductivity of the endplate by heating it. As predicted by Eq. (10) and Fig. 2 for large $\nu$, $\omega_r$ increased to approximately $\omega_E$ and $\gamma$ was reduced to roughly $\omega_c/9$. From Eq. (10) this would indicate that $\nu/\omega_c=18.9$. Thus by heating the plasma terminator $\nu/\omega_c$ changed from 1.28 to 18.9, an increase of a factor of 15. We expect $\nu$ for a clean endplate to be given approximately by Eq. (7). Evaluating this expression for $\nu$ we find $\nu/\omega_c\approx25$. This agrees quite well with the best fit value of $\nu/\omega_c=18.9$. The sheath model we have used in deriving Eq. (7) models the sheath response as being purely resistive. It also has a capacitive component, but this is negligible compared with the resistive response.[12,13] The effect of a "dirty" endplate can be modeled as an added resistance so that $\nu_t^{-1}=\nu_0^{-1}+\nu_{EP}^{-1}$, where $\nu_0$ is given by Eq. (7). We will not attempt to derive an expression for $\nu_{EP}$, the endplate contribution to $\nu_t$. The measurement of $k_\parallel$ was done with the plasma terminator cold.

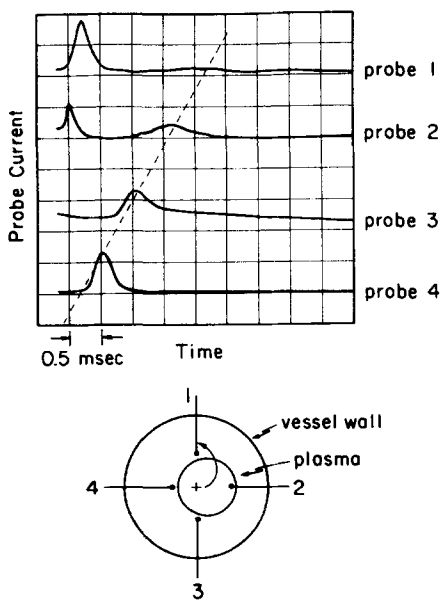


FIG. 4. "Flute" evolution showing $n_i(t)$ at $r=4$ cm and $\theta=0$, 90°, 180° and 270° (top to bottom) at midplane. 500 μsec/div. The lower figure shows the midplane and, schematically, the relative position of the probes, plasma, and vacuum vessel. The plasma is seen to pass through the stationary probes in the sequence 2, 1, 4, 3, 2, and 1. The arrow indicates the direction of motion of the plasma.

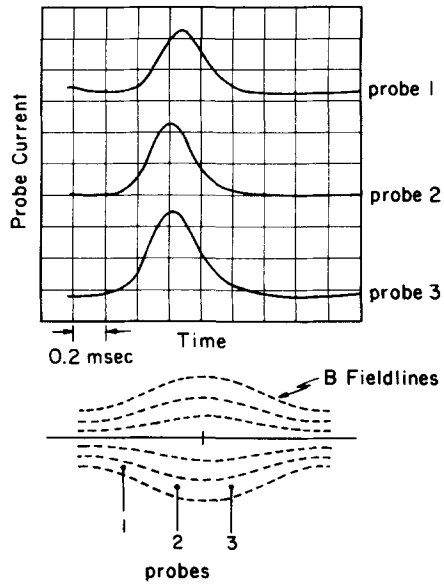


FIG. 5. Mode evolution at three different values of $z$ showing the phase lag between mirror and throat. The top trace is near the peak of magnetic field. The two lower traces are at symmetric positions in the mirror valley. 200 μsec/div. The lower figure shows schematically a side view of the experiment and the relative positions of the probe.

From Eq. (10) it can be shown that the $m=1$ mode does not have the largest growth rate. However, because the plasma is slightly asymmetric, due to the method of plasma production, the $m=1$ mode has a small initial amplitude and thus it is this mode that we observe.

The measurement of $k$ parallel is shown in Fig. 5. The top trace was taken near the throat of the magnetic field and the bottom two traces were taken at symmetric positions near the mirror midplane. The probes were equally spaced along $z$, 23 cm apart, and the radial positions were chosen so that all probes were on the same magnetic field line. The valley probe was at $r=4$. The phase delay estimated from Fig. 5 is approximately 55 μsec between the peak and the valley probes. That delay corresponds to a phase shift of approximately 10°. The value predicted by Eq. (20) is

approximately 3.3° assuming no $\omega_E$ variation. The two valley probes, as expected, show no phase delay. The discrepancy between the theoretical phase shift and the experimentally observed phase shift could be due to variations in $\omega_E$ or line-tying. The phase shift is especially sensitive to any change in $\omega_E$; a change in $\omega_E$ of a few percent could account for the larger observed phase shift. An attempt was made to measure the difference in $\omega_E$, but it was not possible to measure the potential profiles to the degree of accuracy required.

## VI. DISCUSSION AND CONCLUSIONS

We have presented the theory of low-order interchange modes in a cylindrical geometry. The ion response neglects parallel motion, but includes effects due to the wall radius, line tying, finite Larmor radius, and radial electric field. The electron response is non-local and cannot be described by fluid equations.

The $m=1, q=0$ interchange mode has been experimentally observed. The real part of $\omega$ is due to a small amount of line tying and the growth is consistent with the theory that predicts some stabilization due to line tying. When we increased the amount of line tying, the real frequency approached $\omega_E$ and the growth rate was reduced by a factor of 9. A finite $k_z$ was observed, and is due to a finite parallel electron response. We plan further experiments to study the effects of a plasma blanket[14] or surface line tying on the interchange mode.

We have some confidence now in generating and in predicting the properties of the interchange mode in a small axisymmetric mirror. The effects of line-tying have been studied in a controlled manner which is not usually possible in larger experiments. We note, however, that the two values of $\nu/\omega_c$ examined in the experiment do not conclusively verify the theory that we have presented.


## ACKNOWLEDGMENTS

The authors would like to acknowledge useful discussions with Dr. A. Lichtenberg, Dr. M. Lieberman, Dr. N. Rynn, and Dr. D. Segal, and the excellent technical assistance of John Kinley.

The work presented here was supported by the United States Department of Energy.


## APPENDIX

We derive Eqs. (6) and (7) from guiding center drift equations. The treatment here follows Liebermann[12,13] and later Fornaca[15] in its treatment of line-tying. We start with the continuity equation

$$\nabla\cdot\mathbf{J}_1=-\frac{\partial\rho_{e1}}{\partial t}=i\omega\rho_{e1}\,, \tag{A1}$$

where $\mathbf{J}_1=-en_{e0}\mathbf{v}_{e1}-en_{e1}\mathbf{v}_{e0}$ and we identify $-en_{e1}$ as $\rho_{e1}$ and $v_{e0}$ as $r\omega_E\hat{\theta}$, $en_0\mathbf{v}_{e1}$ is made up of the $\mathbf{E}_1\times\mathbf{B}$ drift current plus $J_l$, the line-tying current due to the sheath response at the end wall. There is also a sheath response at the mirror sheath, but it is much smaller and will be neglected here. The line-tying current $J_l$ is found as follows: Because $v_e\gg v_i$, a sheath potential difference $\varphi_0$ at the end plate is required to hold back most of the electrons and thus maintain quasineutrality. Equating the electron and ion currents which leave the plasma we have

$$-J_e=n_0ev_e\exp(-e\varphi/kT_e)=J_i=n_0ev_i\,. \tag{A2}$$

When the potential $\varphi$ in the plasma fluctuates an amount $\varphi_1$ from $\varphi_0$ due to the wave, there is an imbalance in charge flow and a net current results

$$J_l=J_i+J_e=n_0ev_i-n_0ev_e\exp(-e\varphi/kT_e)$$
$$-n_{e1}ev_e\exp(-e\varphi/kT_e)+n_{i1}ev_i\,. \tag{A3}$$

The third term was included by Prater,[4] but he neglected the fourth term on the right-hand side, Eq. (A3). It is the sum of those two terms which may be neglected in comparison to the first two terms. Using the equilibrium condition (A2) the first two terms are

$$J_l=n_0ev_i\,[1-\exp(-e\varphi_1/kT_e)]\approx(n_0e^2v_i/kT_e)\varphi_1\,. \tag{A4}$$

The total perturbed current is

$$\mathbf{J}_1=\rho_1r\omega_E\hat{\theta}-n_0e\,(\mathbf{E}_1\times\mathbf{B}c/B^2)+(n_0e^2v_i/kT_e)\varphi_1\hat{z}\,, \tag{A5}$$

and the divergence of these three terms are, respectively:

$$\nabla\cdot\rho_1r\omega_E\hat{\theta}=\frac{1}{r}\frac{\partial}{\partial\theta}\rho_1r\omega_E=im\omega_E\rho_1\,, \tag{A6}$$

$$\nabla\cdot n_0e\frac{\mathbf{E}_1\times\mathbf{B}c}{B^2}=\nabla n_0e\cdot\frac{\delta\mathbf{E}_1\times\mathbf{B}c}{B^2}$$
$$+n_0ec\mathbf{B}\cdot\nabla\times\mathbf{E}_1+n_0e\mathbf{E}_1\cdot\frac{\nabla\times\mathbf{B}c}{B^2}\,,$$

$$\nabla\cdot n_0e\frac{\mathbf{E}_1\times\mathbf{B}c}{B^2}=\frac{2n_0ecim\varphi_1}{B}\,, \tag{A7}$$

where we have $\nabla\times\mathbf{E}_1\approx0$ because $\beta\approx0$ and also $\nabla\times B=0$, and

$$\frac{\nabla\cdot n_0e^2v_i\varphi_1\hat{z}}{kT_e}=\frac{1}{l_m}\int_0^{l_m}\frac{\partial}{\partial z}\frac{n_0e^2v_i\varphi_1\,dz}{kT_e}=\frac{n_0e^2v_i\varphi_1}{kT_el_m}\,, \tag{A8}$$

$l_m$ is the length of a field line and the average we have taken over a field line in the line-tying term is done because the current that is generated by the sheath fluctuation is distributed along a field line in a time much less than the wave period.[15] Combining these results for the electron response we have

$$\rho_e=-\frac{\epsilon_\perp2m\Omega_i\varphi_1}{4\pi r_0^2\omega}-\frac{in_0e^2v_i\varphi_1}{\omega kT_el_m}$$
$$=\frac{\epsilon_\perp}{4\pi r_0^2}\left[\frac{-2m\Omega_i}{\omega}-\frac{4i}{\omega}\left(\frac{v_ir_0^2\Omega_i^2m_i}{4kT_el_m}\right)\right]\varphi_1\,, \tag{A9}$$

$$\nu=m_iv_i\Omega_i^2r_0^2/4kT_el_m\,.$$

This approximate expression is valid for a clean end-plate. If the end plate is coated with barium, the effective $\nu$ is decreased.


[1] M. N. Rosenbluth and A. Simon, Phys. Fluids 8, 1300 (1965).
[2] J. D. Jukes, Phys. Fluids 7, 1468 (1964).

[3]W. B. Kunkel and J. U. Guillory, in *Proceedings of the Seventh International Conference on Phenomena in Ionized Gases*, Belgrade, 1965, edited by B. Petrovic and D. Tosić, (Gradjevinska Knjiga Publishing House, Belgrade, Yugoslavia, 1966), Vol. II, p. 702.
[4]R. Prater, Phys. Fluids **17**, 193 (1974).
[5]E. Kamke, *Differential Gleichunger* (Chelsea Publishing Company, New York, 1948), 473.
[6]M. N. Rosenbluth, N. A. Krall, and N. Rostoker, Nucl. Fusion Suppl. **143** (1962).
[7]T. D. Rognlien, J. Appl. Phys. **44**, 3505 (1973).
[8]J. C. Riordan and C. W. Hartman, Phys. Fluids **20**, 1378 (1977).
[9]N. Rynn, Rev. Sci. Instrum. **35**, 40 (1964).
[10]B. McVey, Bull. Am. Phys. Soc. **24**, 992 (1979) and M. Musetto, Bull. Am. Phys. Soc. **24**, 992 (1979).
[11]D. Hill, M. Wickham, and S. Fornaca, Bull. Am. Phys. Soc. **24**, 985 (1979).
[12]M. A. Lieberman, Lawrence Livermore Laboratory Report No. UCID-16736 (1976), edited by R. W. Moir, Appendix.
[13]M. A. Lieberman and S. K. Wong, Plasma Phys. **19**, 745 (1977).
[14]S. Fornaca, Y. Kiwamoto, and N. Rynn, Phys. Rev. Lett. **42**, 772 (1979).
[15]S. Fornaca, Ph.D. thesis, University of California, Irvine (1980).